

Switching between impacting and non-impacting co-existing attractors via intermittent control

Dimitri D. A. Costa¹, Vahid Vaziri², Marcelo A. Savi¹, Marian Wiercigroch²

¹*Universidade Federal do Rio de Janeiro, COPPE,
21.945.972, Rio de Janeiro, Brazil*

dda.costa@mecanica.coppe.ufrj.br, savi@mecanica.coppe.ufrj.br

²*Centre for Applied Dynamics Research, School of Engineering, University of Aberdeen, King's College,
Scotland, Aberdeen AB24 3FX, United Kingdom*

Abstract. Multistability manifests itself in several nonlinear systems and structures including origamis, energy harvesters, oil well drilling and microelectromechanical systems. In some applications, this effect is a desired aspect that brings adaptability but in others, only a specific configuration is useful. In all cases, the ability to exchange between undesired and desired responses is crucial for the system proper operation. Usually, this configuration change occurs in a quasi-static framework where the system operation is required to halt for reconfiguration, leading to losses of productivity and waste of time. Hence, control techniques that can transfer between coexistent orbits in a dynamical framework are required. However, there are only a few studies that tackle the control of multi-stable systems, with most controllers only working in the vicinity of the desired behaviour. This work aims to study the intermittent control application from numerical and experimental points of view and analyse its properties in a realistic scenario where noise is present. An experimental impact oscillator is used as a standard multi-stable system. Results show that the controller presents difficulties to exchange coexistent orbits when noise is considered, needing high control gains.

Keywords: Impact oscillator, control, multistability.

1 Introduction

Multi-stability is present in several systems in applied sciences. It has been observed in drill-string dynamics as in De Moraes and Savi [2], the typical two-bar truss system as in Costa *et al.* [3], impact systems as in Ing *et al.* [4], among others. The multi-stability phenomenon is observed in situations where the system response gravitates towards one or more attractors depending on the initial conditions. Multi-stability can be desired and even designed as in origami structures following the work of Kuribayashi *et al.* [5]. In other systems the effect of multi-stability may be dangerous to its operation as in seismic mitigation, or even reduce or render the system effectiveness on its use as in the system presented by Skeem *et al.* [6].

Multi-stability is a typical nonlinear phenomenon and impact oscillator is an emblematic example. The works developed by Ing *et al.* [4], [7]–[9] showed that these systems present a rich dynamics and multi-stability, especially near grazing bifurcations where attractors with a different number of impacts per cycle coexist. These systems are also used to model all sorts of operations as in the work of Wiercigroch and Budak [10] that studied impact effects in machining, in the work of Wiercigroch [11] that uses impacts and resonance to improve drilling process, among others.

The ability to control the system response and choose which of the coexisting attractor is better for operation is crucial. With this in mind, Liu *et al.* [1] proposed the intermittent control which is designed to perform the exchange between co-existent attractors. However, there are very few studies in the literature that apply or study this control method. Hence, this works try to few that gap and study the application of the intermittent control in an experimental impact oscillator and how it performs in a real scenario where noise is

present.

2 Control method

The intermittent control is one of the few methods that is designed to perform exchange between coexisting orbits. Its main idea is to promote the exchange by the elimination of the initial attractor dynamics and the introduction of the desired response dynamics with a proportional feedback gain signal, after a defined criterion is met. This idea is highly successful and ideally is always able to perform the exchange if the criterion is met. It is important to highlight that the desired behaviour is also an attractor of the system and the idea here is just to perform the exchange between one solution of the system to another.

The control signal can be defined by considering an evolution function $f(\mathbf{x})$ of an observable system leading to:

$$\mathbf{u} = -\mathbf{f}_{dyn}(\mathbf{x}, \mathbf{x}_{targ}) - \mathbf{K}\mathbf{e}, \quad (1)$$

where \mathbf{x}_{targ} is the desired behaviour of the system, \mathbf{K} is a positive definite proportional gain matrix, $\mathbf{e} = \mathbf{x} - \mathbf{x}_{targ}$ is the error and \mathbf{f}_{dyn} is the difference between the dynamics of the target behaviour and the dynamics of the system response defined as:

$$\mathbf{f}_{dyn} = \mathbf{f}(\mathbf{x}) - \mathbf{f}(\mathbf{x}_{targ}), \quad (2)$$

The first term of Eq. (1) inputs the desired dynamics into the system while eliminating the current behaviour. The last term of the equation is a proportional feedback used to bring the system response closer to the desired behaviour basin of attraction.

The verification of the control success can be done by differentiating the error with respect to time obtaining the error evolution:

$$\dot{\mathbf{e}} = -\mathbf{K}\mathbf{e}, \quad (3)$$

which has an exponential decaying solution if \mathbf{K} is a positive definite matrix. Hence, as the error tends to zero the system will always converge to the desired response.

Even though the control law of Eq. (1) can exchange between any given pre-existent orbit, its direct application may not be the best solution or even possible in a real application. Restrictions may be in place such as limitations on energy consumption or control signal or even velocity of actuation. Hence, a criterion may be adopted to minimize energy consumption, limit control signal or a combination of these factors so the control can minimize its effort to perform the exchange.

A good strategy is to see at which point of the initial orbit the controller will consume the least energy to perform the exchange. Another strategy is to wait for the system to be at or near the closest point to the desired behaviour and apply the control at that point. One example of this strategy would be waiting for the system state to be at a certain trigger distance $\delta_{trigger}$ from the target orbit, resulting in the following control law:

$$\mathbf{u} = \begin{cases} \mathbf{0} & , \text{if } |\mathbf{x} - \mathbf{x}_{targ}| > \delta_{trigger} \\ -\mathbf{K}\mathbf{e} - \mathbf{f}_{dyn}(\mathbf{x}, \mathbf{x}_{targ}) & , \text{if } |\mathbf{x} - \mathbf{x}_{targ}| < \delta_{trigger} \end{cases}. \quad (4)$$

If the criterion defined in Eq. (4) is used and the system can meet it at some instant, the controller will ideally always bring the system to the desired response. However, if there is any restriction imposed on the control, such as a limited control signal, one of two outcomes is expected: the controller manages to transfer the system to the target attractor by one or more successive act and wait periods that depend on the criteria or the controller cannot transfer the system to the target attractor due to its limitations as it cannot prevail over the current attractor stability. Finally, it is very important to highlight that as the target behaviour is a response of the system the control signal will always tend to zero after the exchange is performed, and hence it will not consume energy afterwards.

The intermittent control is very effective to exchange between behaviours, however, it requires a considerable amount of knowledge about the system and its robustness to model discrepancies or noise was not yet studied. To calculate the control, one needs a time evolution model of the system \mathbf{f} , the knowledge of the system current state \mathbf{x} and the full knowledge of the target orbit \mathbf{x}_{targ} , as well as the phase of the excitation for non-autonomous systems. Hence, on a real implementation, these requirements can lead to high costs, the

introduction of a delay in the control signal due to the required calculations or even the inability of the controller to promote the exchange.

3 Impact oscillator

The specific description of the experimental apparatus and its design is presented in Wiercigroch *et al.* [9], while the configuration utilized in this work is given in Fig. 1. The oscillator is constructed upon a base that provides alignment of components and stability. There is also a stabilizing rigid structure mounted on the base to suppress any spurious external vibrations to the system that may affect the main mass (highlighted in grey). The leaf springs (highlighted in red) are clamped in one end between the mass and two grooved plates, and in the other end between a grooved base and two beams. This ensures proper alignment of the leaf springs. A permanent neodymium magnet is attached to one side of the mass by a stainless steel rod and fixed by two stainless steel nuts that can be adjusted. The magnets position is adjusted to be inside an in-house built coil (highlighted in orange), capable of generating a variable magnetic field that provides direct excitation to the mass due to the magnetic coupling of the coil and magnet. The inner diameter of the coil is close to the diameter of the cylindrical magnet to improve the coupling between the varying field of the coil and the fixed field of the magnet, thereby limiting the nonlinear effects in the excitation system. The current I running through the coil is provided by an NI[®] PCI-6251 board which produces the desired signal and afterwards is amplified by a signal an in-house built amplifier plugged to two current generators. There are impact beams (highlighted in pink) on both sides of the main mass that can be inserted independently. The distance g between an impact beam and the main mass can be easily modified by a treaded bolt fixed to the tip of the beam.

The data is collected by sensors attached to a NI[®] PCI-6251 board and an in-house LabVIEW[®] program. The displacement of the main mass is measured by an eddy current probe (highlighted in light blue) attached to the structure close to the leaf springs base. Accelerometers (highlighted in light blue) are placed on the structure, mass and impact beam, while the coil input is measured by a multi-meter, as shown in Fig. 1. Finally, a piezoelectric load-cell (highlighted in light blue) is placed between the structure and coil to measure the reaction force due to the mass excitation.

The displacement X of the oscillating mass can be calculated by treating the system as a piecewise linear oscillator if $|X| < 6$ mm. Hence, it is considered that the system can be described by:

$$\ddot{X} = -\frac{k_1}{m}X - \frac{k_2}{m}(X - g)H_s(X - g) - \frac{c}{m}\dot{X} + \frac{F_{coil}(t)}{m}, \quad (5)$$

where H_s is a Heaviside step function, k_1 is the stiffness of the leaf springs, k_2 is the stiffness of the impact beam, c is an equivalent damping of the system, dot represents derivatives in relation to time and F_{coil} is the force applied by the coil to the system. Considering that the applied by the coil is a composition of the control signal and a sinusoidal excitation Eq. (5) becomes:

$$\ddot{X} = -\frac{k_1}{m}X - \frac{k_2}{m}(X - g)H_s(X - g) - \frac{c}{m}\dot{X} + \frac{A}{m}\sin(2\pi ft) + \frac{u}{m}, \quad (6)$$

where A is the excitation amplitude, f is the frequency of the excitation, and u is the control signal.

Finally, if non-dimensional units are taken the equation of motion becomes:

$$x'' = -x - \kappa(x - 1)H_s(x - 1) - c^*x' + A^*\sin(f^*t^*) + u^*, \quad (7)$$

where $x = X/g$, $t^* = \omega_0 t$, $\omega_0 = \sqrt{k_1/m}$, $c^* = c/\sqrt{k_1 m}$, $\kappa = k_2/k_1$, $A^* = A/(k_1 g)$, $f^* = 2\pi f/\omega_0$, $u^* = u/(k_1 g)$, and prime represents derivatives in relation to time t^* . This leads to the evolution of the system to be given by:

$$f(x) = \begin{bmatrix} x' \\ -x - \kappa(x - 1)H_s(x - 1) - c^*x' + A^*\sin(f^*t^*) + u^* \end{bmatrix} \quad (8)$$

where $\mathbf{x}' = [x, x']^T$.

The control gain u is then given by the intermittent control with a gain matrix described by:

$$K = \begin{bmatrix} 0 & 0 \\ K_p & K_v \end{bmatrix}, \quad (8)$$

where, $K_p > 0$ and $K_v > 0$ are the scalar gains related to displacement and velocity, respectively.

It is important to highlight that the control updates its signal at least 100 times faster than the excitation of the system which allows the consideration of a continuous actuation in the experiments. However, the velocity signal that is taken by differentiating the position signal of the eddy current probe has a high noise to signal ratio. Due to the high requirements on the update frequency of the control signal no filter is used in the velocity signal as it would slow the experimental program and lower the actuation frequency.

The parameters used in the model are published in literature by Costa *et al.* [13] and are summarized on Tab. 1.

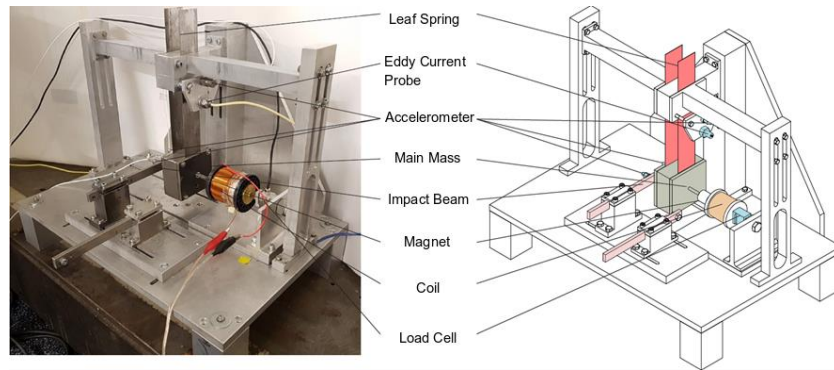


Figure 1. Schematic diagram (right) and the corresponding photograph (left) of the experimental rig. The main components of the system are highlighted as: sensors (eddy current probe, piezoelectric load cell and accelerometers mounted on the mass, frame and impact beam) in blue, coil in orange, main mass in grey, impact beams in pink, leaf springs in red and permanent magnet in white (Costa *et al.*, 2020).

Table 1. Piecewise linear model parameters of the impact oscillator rig.

Parameter	Value	Parameter	Value
g	0.74 mm	k_1	4331 N/m
m	1.325 kg	k_2	87125 N/m
c	0.272 kg/s ²	A	1.16 N

Initially, the dynamics of the oscillator is verified so regions of multi-stability can be identified and used to define the scenarios for the exchange between co-existent attractors. Hence, experimental bifurcation diagrams are traced by increasing and decreasing sweeps of frequency after initializing the system in different initial conditions. The two forward and one backward diagrams that can represent most of the system dynamics and are used for this work can be seen in Fig. 2. Several behaviours can be identified including chaotic orbits and the coexistence of attractors. In fact, coexistence is present from low values of frequency up to 7.1 Hz near the first grazing bifurcation, where a period-1 non-impacting and a period-2 impacting orbit coexists (Fig. 2b) Afterwards, a small window of coexisting chaotic and periodic orbit s exists near grazing. On frequencies above the chaotic region, a period-5 with three impacts per period and period-2 orbit coexists (Fig. 2c). After one of the inner loops of the period-5 orbit suffers grazing incidence the orbit becomes unstable and gives rise to another period-5 orbit now with only two impacts per period (Fig. 2d) that still coexist with the period-2 orbit. Continuing to raise frequency makes the new period-5 orbit unstable due to grazing incidence of one of its loops and only the period-2 orbit is verified. Finally, the diagrams present a chaotic region (Fig. 2e) followed by a period-1 orbit.

The cases are chosen to be very different scenarios so a more general view of the applied control could be achieved. The first one at 6.8 Hz frequency is a test to see if the intermittent control can exchange between impacting and non-impacting coexistent orbits which are very different and crucial behaviour on real applications such as vibro-impact drilling or machining. The second scenario chosen at 7.3 Hz tests if the control method has any difficulty to exchange between higher period orbits.

4 Exchange between coexistent attractors

The intermittent control is tested both numerically and experimentally on each of the two cases. Numerical results are obtained by integrating Eq. 8 by a fourth order Runge-Kutta method with a precision of at least 10^{-6} .

The case at 6.4 Hz is studied by initializing the system on the impacting period-2 orbit and afterwards applying the intermittent control with the period-1 non-impacting orbit as the target. After a successful exchange, the control target is changed again now targeting the period-2 impacting orbit. The gains for the system are set by trial and error numerically and are $K_p = 60.37$ N/m and $K_v = 62.73$ Ns/m for both orbits. After that, the same gains are used in the experiment, however, due to a high noise to signal ratio on velocity, stabilization was not achieved. Hence, the procedure of the control was modified, so it is turned off after a brief period of time that is enough to push the system to the basin of attraction of the targeted attractor.

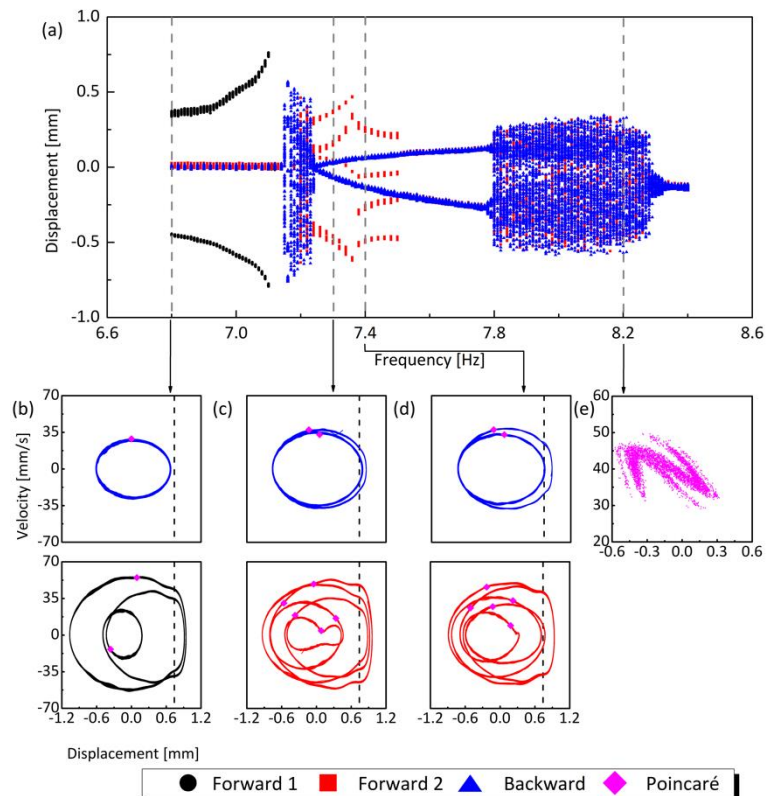


Figure 2. Experimental bifurcation diagram and selected state spaces. Dashed grey lines represent the frequencies where the state spaces are taken and dashed black lines represent the impact boundary. Phase diagrams (b-e) are taken at $f = 6.8, 7.3, 7.4$ and 8.18 Hz respectively.

Figure 3 shows the results for the 6.8 Hz case. In the numerical simulation (Fig. 3a-d) both exchanges are performed by the controller in only one excitation cycle and without any issues. Even though, the control signal has a high peak value, it quickly reduces to zero as the exchange is completed. In experimental results (Fig. 3e-h) the controller can also perform the exchange. The control signal has also a peak of actuation, however, due to the experimental procedure; it only transfers the system from the initial basin of attraction to the basin of the desired behaviour. Hence, after the controller is turned off, the system takes a longer time to converge to the desired orbit when compared to numerical results.

Overall this scenario demonstrates that the intermittent is effective in promoting the exchange between impacting and non-impacting attractors both numerically and experimentally, however it can have problems to perform the exchange if a high noise to signal ratio is present.

The next scenario at 7.3 Hz is also explored with a similar control strategy. The system is initialized in the period-5 orbit, then the controller is turned on targeting the period-2 orbit. After a successful transfer, the control targets the period-5 orbit again. The gains for the system are set by trial and error numerically and are $K_p = 8$ N/m and $K_v = 3.2$ Ns/m when targeting the period-2 orbit and, $K_p = 159.86$ N/m and $K_v = 3.2$ Ns/m on the exchange to the period-5 orbit. In this case, a criteria was introduced so the intermittent control would only start

actuation only if the displacement x of the mass at the Poincaré section is less than 0.1 mm from the other orbit displacement x_{targ} . In other words, the system must obey the restriction $|x - x_{targ}| < 0.1$ mm to turn on. Finally, the control is turned off after the system reaches the target basin of attraction.

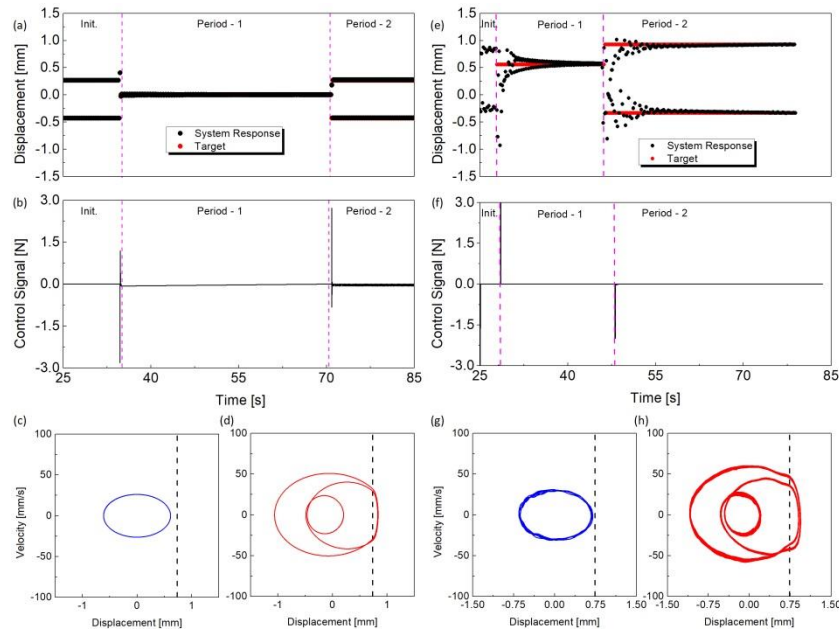


Figure 3. (a-d) Numerical results and (e-h) experimental results at the 6.8 Hz case. Dashed vertical magenta lines represent the exact moments when the controller change its target orbit, while dashed black lines represent the impact boundary. (a)(e) Poincaré stroboscopic time history of position. (b)(f) Control signal time history. (c)(g) Numerical and experimental targeted period-1 orbit respectively. (d)(h) Numerical and experimental targeted period-2 orbit respectively.

Figure 4 shows the results for the 7.3 Hz case. In numerical results (Fig. 4a-d), the controller can perform the exchange without issues, however, due to the low K_v the control takes around five periods of excitation to perform the exchange instead of just one. The lower gains also reflect on the control signal that is one order of magnitude smaller than the 6.8 Hz case. In experimental results (Fig. 4e-h), the control initially targets the period-2 orbit, however, the system moves away from the specified restriction of displacement due to noise. After three windows of actuation, where the system obey de criterion, the desired orbit is reached. On the exchange to the period-5 orbit, the controller only needs one actuation window to bring the system to the desired basing of attraction with a much higher control signal due to the higher gains and is turned off afterwards so the system can converge to the desired orbit.

The case at 7.3 Hz shows that higher gains in the intermittent control raise the control signal and can destabilize the target orbit if noise is present. On the other hand, low control gains may need more than one window of actuation to actually perform the exchange due to noise.

5 Conclusions

This work deals with the implementation of the intermittent control on an impact oscillator that presents several co-existent attractors. The dynamics of the system was investigated and two scenarios were chosen to perform the controlled exchange. While numerical results display a perfect control, experimental results show the vulnerability of the intermittent control to noise. In fact, results show that if noise is present a balance between small and high gains should be reached to avoid multiple windows of actuation or the destabilization of the targeted orbit respectively.

Acknowledgements.

The authors would like to acknowledge the financial support of CNPq, CAPES and FAPERJ.

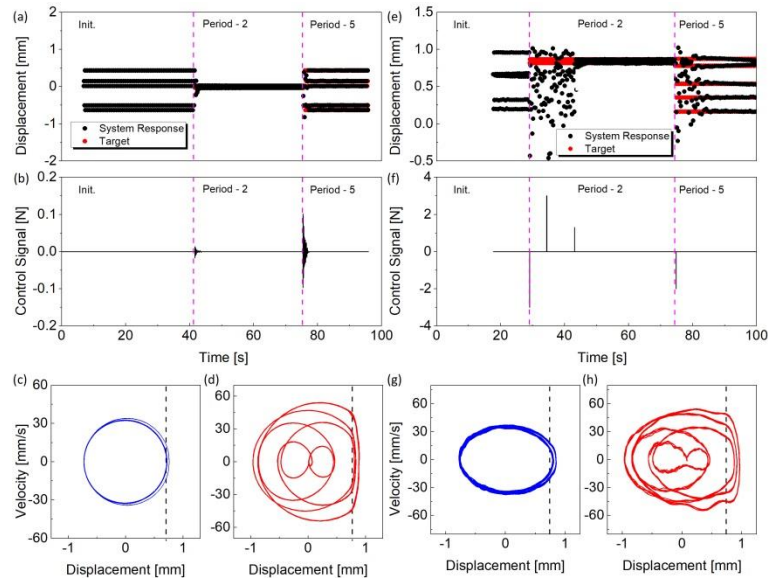


Figure 4: (a-d) Numerical results and (e-h) experimental results at the 7.3 Hz case. Dashed vertical magenta lines represent the exact moments when the controller change its target orbit, while dashed black lines represent the impact boundary. (a)(e) Poincaré stroboscopic time history of position taken on different phase shifts. (b)(f) Control signal time history. (c)(g) Numerical and experimental period-2 targeted orbit respectively. (d)(h) Numerical and experimental period-5 targeted orbit respectively.

Authorship statement.

The authors hereby confirm that they are the sole liable persons responsible for the authorship of this work, and that all material that has been herein included as part of the present paper is either the property (and authorship) of the authors, or has the permission of the owners to be included here.

References

- [1] Y. Liu, M. Wiercigroch, J. Ing, and E. Pavlovskaja, "Intermittent control of coexisting attractors," *Philos. Trans. R. Soc. Math. Phys. Eng. Sci.*, vol. 371, no. 1993, pp. 20120428–20120428, 2013.
- [2] L. P. P. de Moraes and M. A. Savi, "Drill-string vibration analysis considering an axial-torsional-lateral nonsmooth model," *J. Sound Vib.*, vol. 438, pp. 220–237, 2019.
- [3] D. D. A. Costa, M. A. Savi, A. S. De Paula, and D. Bernardini, "Chaos control of a shape memory alloy structure using thermal constrained actuation," *Int. J. Non-Linear Mech.*, 2019.
- [4] J. Ing, E. Pavlovskaja, and M. Wiercigroch, "Dynamics of a nearly symmetrical piecewise linear oscillator close to grazing incidence: Modelling and experimental verification," *Nonlinear Dyn.*, vol. 46, no. 3, pp. 225–238, 2006.
- [5] K. Kuribayashi *et al.*, "Self-deployable origami stent grafts as a biomedical application of Ni-rich TiNi shape memory alloy foil," *Mater. Sci. Eng. A*, vol. 419, no. 1–2, pp. 131–137, 2006.
- [6] M. R. Skeem, M. B. Friedman, and B. H. Walker, "Drillstring Dynamics During Jar Operation," *J. Pet. Technol.*, vol. 31, no. 11, pp. 1381–1386, 1979.
- [7] Q. Cao, M. Wiercigroch, E. E. Pavlovskaja, C. Grebogi, and J. M. T. Thompson, "The limit case response of the archetypal oscillator for smooth and discontinuous dynamics," *Int. J. Non-Linear Mech.*, vol. 43, no. 6, pp. 462–473, 2008.
- [8] J. Ing, E. Pavlovskaja, M. Wiercigroch, and S. Banerjee, "Experimental study of impact oscillator with one-sided elastic constraint," *Philos. Trans. R. Soc. Math. Phys. Eng. Sci.*, vol. 366, no. 1866, pp. 679–705, 2008.
- [9] J. Ing, E. Pavlovskaja, M. Wiercigroch, and S. Banerjee, "Bifurcation analysis of an impact oscillator with a one-sided elastic constraint near grazing," *Phys. Nonlinear Phenom.*, vol. 239, no. 6, pp. 312–321, 2010.
- [10] M. Wiercigroch and E. Budak, "Sources of Nonlinearities, Chatter Generation and Suppression in Metal Cutting," *Philos. Trans. Math. Phys. Eng. Sci.*, vol. 359, no. 1781, pp. 663–693, 2001.
- [11] M. Wiercigroch, "Resonance enhanced drilling: method and apparatus. Patent No. WO2007141550," 2007.
- [12] M. Wiercigroch, S. Kovacs, S. Zhong, D. Costa, V. Vaziri, M. Kapitaniak and E. Pavlovskaja, "Versatile mass excited impact oscillator," *Nonlinear Dyn.*, vol. 99, no. 1, pp. 323–339, 2020.
- [13] D. Costa, V. Vaziri, M. Kapitaniak, S. Kovacs, E. Pavlovskaja M. A. Savi and M. Wiercigroch, "Chaos in impact oscillators not in vain: Dynamics of new mass excited oscillator," *Nonlinear Dyn.*, 2020.